Am J Transl Res 2026;18(4):2951-2963
www.ajtr.org /ISSN:1943-8141/AJTR0168543

Original Article

Value of dual-energy CT parameters DER and DEI in predicting calcium-containing urinary stones and differentiating pure calcium oxalate monohydrate

Bin Hou, Qiong Zheng

Department of Radiology and Medical Imaging, Lanzhou Petrochemical General Hospital (The Fourth Affiliated Hospital of Gansu University of Chinese Medicine), No. 733, Fuli West Road, Xigu District, Lanzhou 730060, Gansu, China

Received September 3, 2025; Accepted January 21, 2026; Epub April 15, 2026; Published April 30, 2026

Abstract: Objective: To investigate the diagnostic value of quantitative parameters (including dual-energy ratio (DER) and dual-energy index (DEI)) from dual-source dual-energy computed tomography (DECT) in predicting calcium-containing urinary stone subtypes and differentiating pure calcium oxalate monohydrate (COM) stones. Methods: We conducted a retrospective analysis of 311 patients with urinary stones diagnosed between May 2022 and September 2024, including 119 patients with uric acid (UA) stones and 192 patients with non UA calcium-containing stones according to Fourier-transform infrared spectroscopy. All patients underwent DECT, and CT attenuation values were measured on virtual monoenergetic images at 40 keV and 80 keV. Multiple parameters were calculated from these measurements: dual-energy density (DED), DER, DEI, and effective atomic number (Eff-Z). Infrared spectroscopy was used as the gold standard for stone composition analysis. ROC curve analysis was used to test the diagnostic efficacy of CT-based parameters. A confusion matrix was then constructed to comprehensively evaluate diagnostic performance, including sensitivity, specificity, and accuracy. Results: When evaluating the ability of various imaging parameters to differentiate between uric acid stones and calcium-containing stones, Eff-Z demonstrated the strongest discriminative ability, with an AUC of 0.938 and an accuracy of 88.42%. DER and DEI followed closely, with slightly lower diagnostic efficacy but still significant. In the comparison between COM and non-COM stones, after adjusting for orientation, DER (AUC 0.854, accuracy 80.21%) and DEI (AUC 0.760, accuracy 70.31%) still provided effective differential diagnostic criteria. There were statistical differences in DER and DEI measurements (both P<0.001). Conclusion: DER, DEI, and Eff-Z from dual-source CT can effectively differentiate between uric acid stones and calcium-containing stones, with Eff-Z being the best indicator. DER and DEI can further help identify pure COM stones, providing value for preoperative non-invasive assessment.

Keywords: Dual-source dual-energy computed tomography, dual-energy ratio, dual-energy index, effective atomic number, urinary stone composition, calcium oxalate monohydrate

Introduction

Urolithiasis has a very high prevalence, reaching 10%-15% in some regions, posing a significant public health burden [1]. The disease is characterized by frequent recurrences and diverse stone compositions, and is significantly associated with metabolic disorders, dietary habits, and environmental factors [2]. Understanding the type of stone is crucial as it affects disease progression, physician decisions, the probability of recurrence, and the likelihood of disease exacerbation. Uric acid (UA) stones usually respond well to urine alkalization or drug dissolution, while calcium oxalate and calcium phosphate stones often require extracorporeal shock wave lithotripsy or surgical intervention [3]. Therefore, determining the composition of the stone - ideally without surgery - is an important step in developing personalized treatment plans.

The definitive identification of stone composition still relies primarily on postoperative specimen analysis, such as infrared spectroscopy or chemical analysis. While these methods are highly accurate, they are only applicable to the postoperative stage and lack preoperative

https://doi.org/10.62347/RHOT8564

value [4]. Traditional computed tomography (CT), while providing stone density information in Huntsfield units, has significant limitations in distinguishing different stone types [5]. For instance, some UA stones and calcium oxalate stones have overlapping CT values, making them difficult to distinguish based on a single parameter. This problem is even more pronounced when differentiating calcium oxalate subtypes, including pure calcium oxalate monohydrate (COM) from calcium oxalate dihydrate (COD) and calcium phosphate (CaP), which greatly limits the role of imaging in preoperative prediction of stone composition [6]. Dual-energy CT (DECT) has now become an important non-invasive method for examining stone composition [7]. By acquiring CT values at different energy levels and using spectral curve analysis, DECT can calculate multiple quantitative parameters, such as DED, DER, DEI, and Eff-Z [8]. These indicators help distinguish the main components of stones and their chemical and physical properties. Previous studies have shown that DECT has high sensitivity and specificity in distinguishing UA stones from calcium-containing stones. For example, Kaviani et al. [9] found that the area under the curve (AUC) for this distinction was 0.78, which supports its application in medicine. Nonetheless, research on the evaluation of DECT for identifying calcium-containing stone subtypes (especially pure COM) remains insufficient.

COM is one of the most common types of urolithiasis, accounting for approximately 70%-80% of calcium oxalate stones [10]. It has high hardness and density, poor response to lithotripsy, and is associated with a higher risk of recurrence [11]. In contrast, COD and CaP stones differ in radiographic features and clinical management. Therefore, accurate preoperative radiographic identification of COM stones is crucial for clinical decision-making and prognosis. Against this backdrop, this study explored the composition of urolithiasis using quantitative parameters from dual-source CT, focusing particularly on the value of these parameters in identifying calcium-containing stone subtypes (especially pure COM). By analyzing radiographic features, this study aims to provide a basis for non-invasive stone composition identification and support more precise preoperative assessment and individualized treatment. This study aims to provide a basis for non-invasive stone composition identification by analyzing imaging features, and to support more accurate preoperative assessment and individualized treatment.

Methods and materials

Sample size assessment

To evaluate the value of dual-source CT parameters (DER and DEI) in predicting calcium-containing urinary stone subtypes and differentiating pure COM stones, sample size was estimated based on receiver operating characteristic (ROC) curve calculation. We referenced the study by Kaviani et al. [9], in which the reported area under the curve (AUC) value of 0.78 was used as a model performance index to distinguish UA stones from calcium-containing stones. Based on this, we set the significance level (α) at 0.05 and target statistical power ($1-\beta$) at 0.80. Additionally, according to literature data and using the pROC package in R language, approximately 15 cases were required per group. Therefore, the recommended total sample size was 30 cases. Finally, based on available clinical resources, we collected clinical data from 311 patients with urinary stones.

Sample collection

This retrospective study collected data from 311 patients with urinary stones treated at Lanzhou Petrochemical General Hospital between May 2022 and September 2024. The study was approved by the Medical Ethics Committee of Lanzhou Petrochemical General Hospital.

Inclusion and exclusion criteria

Inclusion criteria: Stones confirmed by infrared spectroscopy to be UA stones, calcium-containing stones (calcium oxalate, calcium phosphate), or non-calcium-containing stones; stone removal surgery conducted within one month of diagnosis, with sufficient specimen volume to ensure reliable infrared spectroscopy results; CT image quality meeting diagnostic and post-processing analysis standards; patient age ≥18 years, with complete clinical and imaging data.

Exclusion criteria: Stone diameter ≤5 mm, insufficient to ensure accuracy of component analysis and imaging measurements; poor image quality or incomplete images with severe artifacts, not meeting diagnostic and post-processing requirements; stone composition not

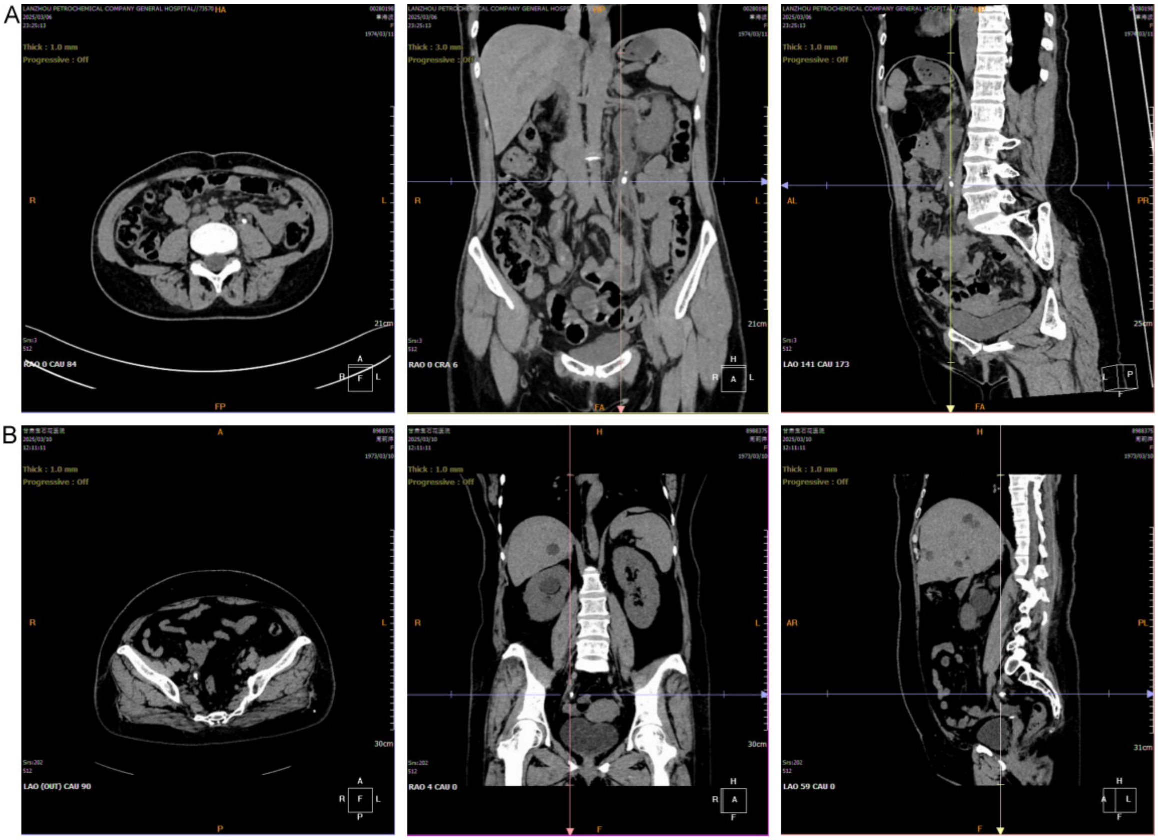

Figure 1. Representative dual-source CT images of two urinary stone patients. A: Female, 51 years old. Axial, coronal, and sagittal reconstruction images demonstrate a stone located in the right upper urinary tract (ureter/renal pelvis region), appearing as localized high-density shadow. B: Female, 52 years old. Axial, coronal, and sagittal reconstruction images show a stone in the lower urinary tract (bladder/distal ureter region), presenting as a localized high-density shadow.

belonging to the calcium-containing stones required for analysis in this study; previous urological surgery or extracorporeal shock wave lithotripsy resulting in incomplete stone specimens or only residual fragments.

Imaging examination

All subjects emptied their bladders before the examination and underwent a DECT scan of the urinary system in a supine position. The scan was performed using a dual-source spiral CT scanner (model: SOMATOM Inition Flash), with the scanning range from the upper pole of the kidney to the base of the bladder. The main scanning parameters were: dual-energy mode, simultaneous acquisition at 80 kV and 140 kV tube voltages, tube current automatically adjusted according to body size (250-350 mAs), pitch 0.5-0.6, slice thickness and interslice spacing both 0.6 mm, and matrix 512×512. To reduce motion artifacts, all patients cooperated by holding their breath during the scan.

Raw image data was transmitted to a workstation (model: MCL-D2618), and spectral analysis was performed using dedicated dual-energy post-processing software. Spectral curves of the stones were plotted, CT values at 40 keV and 80 keV were measured, and DER, DEI, DED, and Eff-Z were automatically calculated. All measurements were independently performed by two radiologists with associate chief physician qualifications or above; in case of disagreement, a third expert made the final decision. The obtained parameters were used to compare the spectral characteristics of different stone types and evaluate the value of dual-source CT in the differential diagnosis of UA stones, calcium-containing stones, and calcium-containing stone subtypes (**Figure 1**).

Infrared spectroscopy detection methods

All stone specimens were obtained surgically or naturally. After collection, they were rinsed with physiological saline to remove surface blood and debris, and then air-dried at room temperature. The dried stones were mechanically pulverized and ground into a uniform fine powder.

Laboratory testing was performed using a Fourier transform infrared spectrometer (Nicolet iS20). Approximately 1-2 mg of stone powder was mixed with 150-200 mg of anhydrous potassium bromide (KBr), ground uniformly, and pressed into translucent thin films with a diameter of approximately 1 mm. Each sample was scanned three times in the wavenumber range of 4,000-400 cm^{-1} to ensure its stability. The obtained spectra were compared with a standard spectral library, and the main chemical components were determined using characteristic absorption peaks. This method can distinguish subtypes of UA, COM, COD, and CaP, as well as their mixing ratios. Infrared spectroscopy is the best method for determining the composition of stones and is also used to compare the consistency and diagnostic performance of dual-source CT parameters.

Assessment of inter-observer agreement

Based on independent measurements by two radiologists on 50 randomly selected cases, Cohen's kappa coefficient was used to assess the inter-observer consistency of key parameters (DER, DEI, and Eff-Z). To evaluate measurement reproducibility, two radiologists independently performed parameter measurements (dual-energy ratio, dual-energy index, and effective atomic number (Eff-Z)) in 50 randomly selected cases. Inter-observer agreement was assessed using Cohen's kappa coefficient with 95% confidence intervals, and statistical significance was defined as P<0.05.

Clinical and imaging data collection

Study data were retrospectively collected from the hospital's electronic medical record system and PACS. Complete clinical and imaging information for all included patients was obtained. Clinical variables included demographics (age, sex, body mass index), disease-related details (lesion location, family history, stone composition), comorbidities (hypertension and diabetes), and lifestyle factors (smoking and alcohol consumption history). Stone composition was verified by infrared spectroscopy analysis and categorized as UA or non-UA, with non-UA stones further divided into COM, COD, CaP, and mixed types such as COM+COD, COM+CaP, and COM+COD+CaP.

Imaging data were obtained from dual-source CT scans performed according to a standardized protocol. Images were transmitted via PACS for spectral post-processing, recording CT values at 40 keV and 80 keV, as well as quantitative parameters (DED, DER, DEI, Eff-Z). All measurements were performed independently by two experienced radiologists, and any discrepancies were adjudicated by a third senior radiologist. All clinical and imaging data were anonymized before being entered into the analysis database.

Statistical analysis

All data were analyzed using SPSS version 27.0 (IBM, Armonk, USA) and R language version 4.3.3 (R Foundation for Statistical Computation, using the pROC package). The Kolmogorov-Smirnov (KS) test was used to test the normality of continuous variables before analysis. Normally distributed data were expressed as mean ± standard deviation ($\overline{x} \pm s$), and independent samples t-tests were used for comparisons between groups. Non-normally distributed data were expressed as median and interquartile range [M (Q1, Q3)], and Mann-Whitney U tests were used for comparisons between groups. Categorical variables were expressed as frequency and percentage, and chi-square tests were used for comparisons between groups. To further evaluate the efficacy of dual-source CT quantitative parameters in the differential diagnosis of different stone types, ROC curves were plotted and AUC was calculated, along with the optimal cutoff value, sensitivity, and specificity. To comprehensively evaluate model performance, accuracy, sensitivity, specificity, precision, recall, and F1 score were also calculated based on the confusion matrix. P<0.05 indicated statistical significance.

Table 1. Comparison of general characteristics between patients with non-uric acid and uric acid stones

Variable	Non-Uric Acid Stones (n=192)	Uric Acid Stones (n=119)	Test Statistic	*P*-value
Age	53.89±9.10	54.15±10.41	0.237	0.813
BMI	23.43±4.04	22.69±3.83	-1.598	0.111
Gender			1.195	0.274
Male	131 (68.23%)	74 (62.18%)		
Female	61 (31.77%)	45 (37.82%)		
Lesion Location			0.127	0.721
Upper urinary tract	177 (92.19%)	111 (93.28%)		
Lower urinary tract	15 (7.81%)	8 (6.72%)		
Family History of Stones			1.195	0.274
Yes	61 (31.77%)	45 (37.82%)		
No	131 (68.23%)	74 (62.18%)		
History of Hypertension			0.352	0.553
Yes	29 (15.10%)	21 (17.65%)		
No	163 (84.90%)	98 (82.35%)		
History of Diabetes			0.027	0.87
Yes	23 (11.98%)	15 (12.61%)		
No	169 (88.02%)	104 (87.39%)		
Smoking History			0.284	0.594
Yes	144 (75.00%)	86 (72.27%)		
No	48 (25.00%)	33 (27.73%)		
Drinking History			0.504	0.478
Yes	65 (33.85%)	45 (37.82%)		
No	127 (66.15%)	74 (62.18%)		

Note: BMI: Body Mass Index.

Results

Inter-observer agreement

Inter-observer agreement was good to excellent for the key DECT parameters. The Cohen's kappa values were 0.85 (95% CI: 0.78-0.92) for dual-energy ratio, 0.82 (95% CI: 0.75-0.89) for dual-energy index, and 0.90 (95% CI: 0.85-0.95) for Eff-Z (all P<0.001), indicating high reproducibility across readers.

Comparison of clinical characteristics between non-UA and UA stone patients

There were no statistically significant differences in age (P=0.813) and BMI (P=0.111) between patients with non-UA stones and those with UA stones. There were also no significant differences in gender (P=0.274), lesion location (P=0.721), family history of stones (P=0.274), history of hypertension (P=0.553), history of diabetes (P=0.870), smoking history (P=0.594), and alcohol consumption history (P=0.478) between the two groups (**Table 1**).

Comparison of dual-source CT parameters between UA and non-UA stone patients

In the comparison of dual-source CT parameters, compared with patients without UA stones, patients with UA stones showed significantly lower levels of 40 keV CT values, 80 keV CT values, DED, DER, DEI, and Eff-Z, P<0.001 (**Table 2**).

Efficacy analysis of dual-source CT parameters in differentiating UA from non-UA stones

ROC curve analysis revealed that all dual-source CT parameters demonstrated high diagnostic efficacy in differentiating UA from non-UA stones. Among all parameters, Eff-Z had the largest AUC (0.938), followed by DER (0.889), DED (0.879), 40 keV (0.851), and DEI (0.827), while 80 keV had a lower AUC of 0.668. The

Table 2. Comparison of dual-source CT parameters between patients with non-uric acid and uric acid stones

Variable	Non-Uric Acid Stones (n=192)	Uric Acid Stones (n=119)	Test Statistic	*P*-value
CT (40 KeV)	2364.18 [1889.14, 2795.48]	1276.30 [629.13, 1906.41]	10.415	<0.001
CT (80 KeV)	915.31±271.85	782.32±201.37	4.609	<0.001
DED	381.76 [292.57, 440.44]	150.79 [79.55, 233.49]	11.248	<0.001
DER	1.64±0.22	1.21±0.27	15.224	<0.001
DEI	0.10 [0.08, 0.12]	0.04 [0.02, 0.08]	9.719	<0.001
Eff-Z	13.37±1.68	9.58±1.80	18.814	<0.001

Note: DED: Dual Energy Density, DER: Dual Energy Ratio, DEI: Dual Energy Index, Eff-Z: Effective Atomic Number.

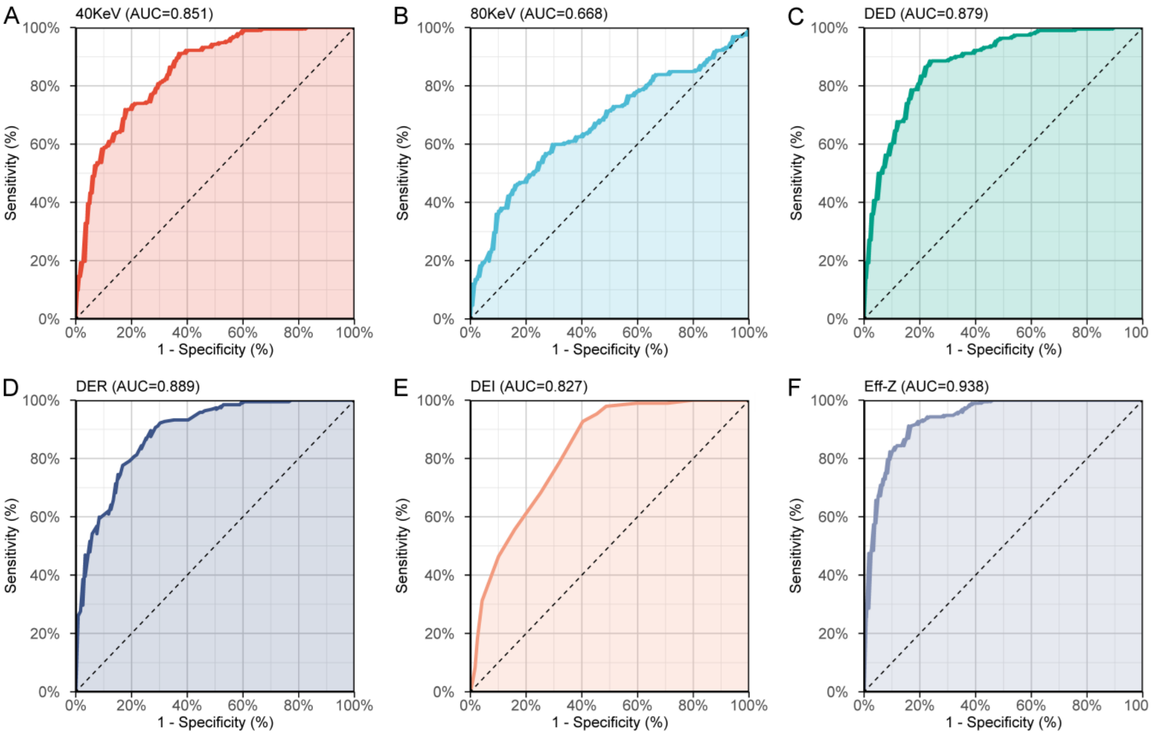

Figure 2. ROC curves of dual-source CT parameters for differentiating uric acid from non-uric acid stones. A: ROC curve for 40KeV spectral CT values (AUC=0.851). B: ROC curve for 80KeV spectral CT values (AUC=0.668). C: ROC curve for DED (AUC=0.879). D: ROC curve for DER (AUC=0.889). E: ROC curve for DEI (AUC=0.827). F: ROC curve for Eff-Z (AUC=0.938). Note: DED: Dual Energy Density, DER: Dual Energy Ratio, DEI: Dual Energy Index, Eff-Z: Effective Atomic Number.

accuracies obtained from the confusion matrix were as follows: Eff-Z (88.42%), DED (83.92%), DER (83.28%), DEI (80.06%), 40 keV (75.88%), and 80 keV (63.99%). Overall, Eff-Z, DER, and DED demonstrated strong and stable performance in differentiating uric acid stones from non-uric acid stones (**Figures 2**, **3**; **Table 2**).

Comparison of general clinical characteristic between COM and non-COM stone patients

In the COM versus non-COM comparison, a significant difference was found only in family history of stones (P=0.044). Age (P=0.703), BMI (P=0.186), gender (P=0.656), lesion location (P=0.495), hypertension (P=0.973), diabetes (P=0.793), smoking history (P=0.735), and alcohol consumption history (P=0.738) (**Table 3**).

Comparison of dual-source CT parameters between COM and non-COM stone patients

In dual-source CT parameter comparisons, the COM stone group showed significantly lower CT (40 keV), CT (80 keV), DED, DER, and DEI levels

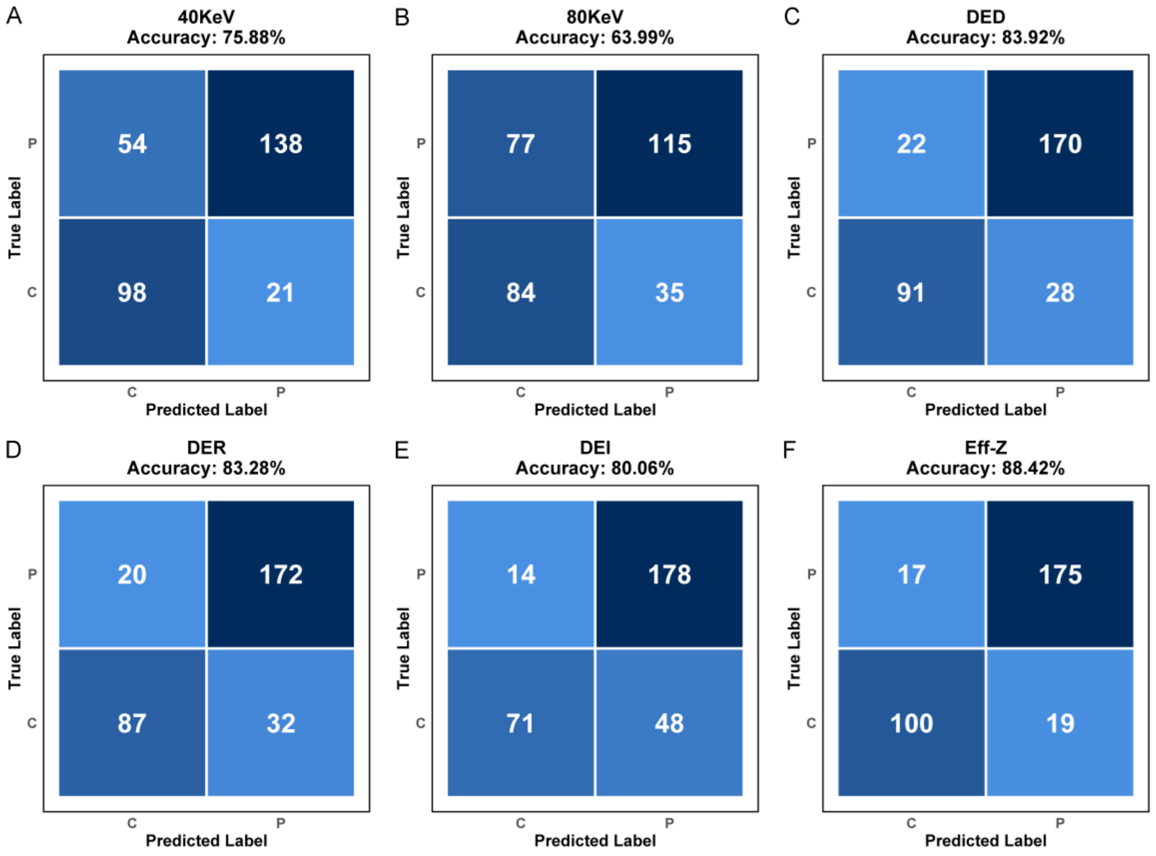

Figure 3. Confusion matrices of dual-source CT parameters for uric acid stones (C) versus non-uric acid stones (P). A: Prediction results for 40 KeV, accuracy =75.88%. B: Prediction results for 80 KeV, accuracy =63.99%. C: Prediction results for DED, accuracy =83.92%. D: Prediction results for DER, accuracy =83.28%. E: Prediction results for DEI, accuracy =80.06%. F: Prediction results for Eff-Z, accuracy =88.42%. Note: DED: Dual Energy Density, DER: Dual Energy Ratio, DEI: Dual Energy Index, Eff-Z: Effective Atomic Number, C: Uric Acid Stone, P: Non-Uric Acid Stone.

Table 3. Diagnostic performance comparison of dual-source CT parameters in differentiating uric acid from non-uric acid stones

Marker	AUC	CI_lower_upper	Accuracy	Sensitivity	Specificity	Precision	Recall	F1-Score	Cut_off
40 KeV	0.851	0.808-0.895	75.88%	71.88%	82.35%	86.79%	71.88%	78.63%	1958.765
80 KeV	0.672	0.612-0.731	64.31%	60.42%	70.59%	76.82%	60.42%	67.64%	885.06
DED	0.879	0.840-0.919	83.92%	88.54%	76.47%	85.86%	88.54%	87.18%	235.295
DER	0.889	0.852-0.926	83.28%	89.58%	73.11%	84.31%	89.58%	86.87%	1.365
DEI	0.827	0.778-0.875	80.06%	92.71%	59.66%	78.76%	92.71%	85.17%	0.065
Eff-Z	0.938	0.910-0.965	88.42%	91.15%	84.03%	90.21%	91.15%	90.67%	11.205

Note: DED: Dual Energy Density, DER: Dual Energy Ratio, DEI: Dual Energy Index, Eff-Z: Effective Atomic Number.

compared to the non-COM stone group (all P<0.001). However, there was no statistically significant difference in Eff-Z between the two groups (P=0.163) (**Table 4**).

Efficacy analysis of dual-source CT parameters in differentiating COM from non-COM stones

ROC curve analysis showed that DER (AUC =0.854) and DEI (AUC=0.760) exhibited high AUC values in differentiating COM from non-COM stones. After orientation correction, DER achieved the highest accuracy (80.21%), followed by DEI (70.31%), 40 keV (72.92%), and 80 keV (68.75%). DED demonstrated a moderate accuracy (69.27%), while Eff-Z showed the lowest accuracy (45.83%). These results indicate that after orientation correction, DER and DEI have good ability to distinguish COM (**Table 5**; **Figures 4** and **5**).

Table 4. Comparison of general characteristics between patients with COM and non-COM stones

Variable	COM (n=80)	Non-COM (n=112)	Test Statistic	*P*-value
Age	53.59±8.52	54.10±9.53	0.382	0.703
BMI	22.97±3.81	23.75±4.18	1.328	0.186
Gender			0.198	0.656
Male	56 (70.00%)	75 (66.96%)		
Female	24 (30.00%)	37 (33.04%)		
Lesion Location			0.465	0.495
Upper urinary tract	75 (93.75%)	102 (91.07%)		
Lower urinary tract	5 (6.25%)	10 (8.93%)		
Family History of Stones			4.07	0.044
Yes	19 (23.75%)	42 (37.50%)		
No	61 (76.25%)	70 (62.50%)		
History of Hypertension			0.001	0.973
Yes	12 (15.00%)	17 (15.18%)		
No	68 (85.00%)	95 (84.82%)		
History of Diabetes			0.069	0.793
Yes	9 (11.25%)	14 (12.50%)		
No	71 (88.75%)	98 (87.50%)		
Smoking History			0.114	0.735
Yes	59 (73.75%)	85 (75.89%)		
No	21 (26.25%)	27 (24.11%)		
Drinking History			0.112	0.738
Yes	26 (32.50%)	39 (34.82%)		
No	54 (67.50%)	73 (65.18%)		

Note: BMI: Body Mass Index, COM: Calcium Oxalate Monohydrate.

Table 5. Comparison of dual-source CT parameters between patients with COM and non-COM stones

Variable	COM (n=80)	Non-COM (n=112)	Test Statistic	*P*-value
CT (40 KeV)	2135.68 [1941.30, 2386.56]	2718.14 [1795.79, 3055.26]	4.673	<0.001
CT (80 KeV)	847.88 [750.79, 944.50]	1014.34 [772.25, 1170.62]	4.358	<0.001
DED	288.95 [233.09, 345.76]	428.51 [391.20, 490.51]	9.98	<0.001
DER	1.49±0.16	1.74±0.20	9.578	<0.001
DEI	0.09 [0.07, 0.10]	0.11 [0.09, 0.13]	6.187	<0.001
Eff-Z	13.57±1.75	13.22±1.62	-1.401	0.163

Note: DED: Dual Energy Density, DER: Dual Energy Ratio, DEI: Dual Energy Index, Eff-Z: Effective Atomic Number, COM: Calcium Oxalate Monohydrate.

Comparison of dual-source CT parameters among different component types of COM

Significant differences in stones were observed in 40 keV (P<0.001), 80 keV (P<0.001), DED (P=0.022), DER (P<0.001), and DEI (P<0.001) among patients with different component types of calcium oxalate monohydrate stones. Among these, DER and DEI showed the most significant differences in distinguishing between different component types. There were no statistically significant differences in Eff-Z among the groups (P=0.223) (**Tables 6** and **7**).

Discussion

Urinary stone disease continues to impose a substantial clinical burden worldwide, with reported prevalence reaching 10%-15% in some regions [12]. In the present study, DECT-derived quantitative parameters demonstrated clear value for non-invasive preoperative character-

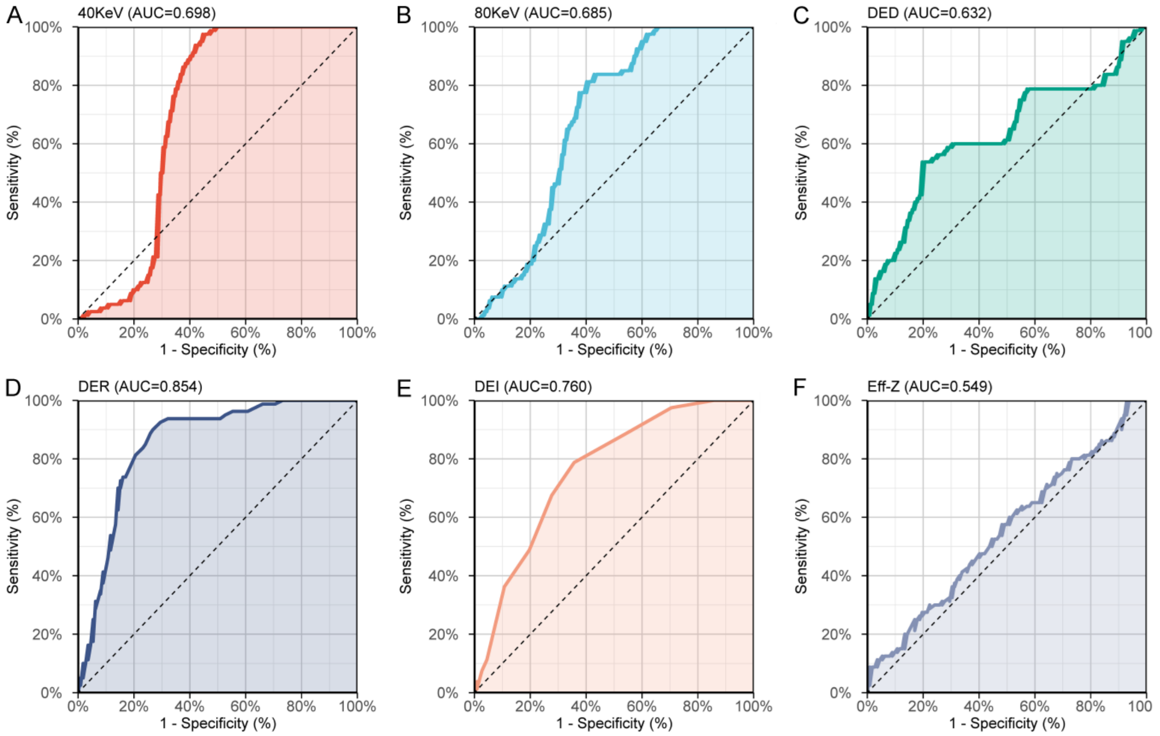

Figure 4. ROC curves of dual-source CT parameters for differentiating COM from non-COM stones. A: ROC curve for 40KeV spectral CT values (AUC=0.698). B: ROC curve for 80KeV spectral CT values (AUC=0.685). C: ROC curve for DED (AUC=0.632). D: ROC curve for DER (AUC=0.854). E: ROC curve for DEI (AUC=0.760). F: ROC curve for Eff-Z (AUC=0.549). Note: DED: Dual Energy Density, DER: Dual Energy Ratio, DEI: Dual Energy Index, Eff-Z: Effective Atomic Number, COM: Calcium Oxalate Monohydrate.

ization of stone composition, addressing a key limitation of conventional single-energy CT, where attenuation overlap between uric acid and calcium-containing stones can compromise discrimination [13]. Our results support a multiparametric approach: Eff-Z provided the strongest separation between uric acid and calcium-containing stones, while DER and DEI offered additional discriminatory information for identifying pure calcium oxalate monohydrate stones. This finding is consistent with prior evidence that combining multiple DECT indices improves diagnostic performance compared with reliance on a single metric, reinforcing the clinical potential of quantitative DECT for individualized treatment planning [14].

This study, through the analysis of 311 patients, confirmed the practicality of DECT quantitative parameters in predicting stone composition. When distinguishing between UA stones and calcium-containing stones, the Eff-Z showed the most significant performance, with an AUC of 0.938 and an accuracy of 88.42%. This result is based on the physical principle that UA stones are composed of light elements such as carbon, hydrogen, nitrogen, and oxygen (C, H, N, and O ($C_4H_4N_4O_3$), whereas calcium-containing stones contain calcium, which has a higher atomic number. Previous studies [15] have shown that Eff-Z reflects these atomic number differences effectively, explaining why Eff-Z serves as a strong distinguishing parameter. DER and DED also demonstrated solid diagnostic ability, with AUCs of 0.889 and 0.879, respectively, and accuracy rates of 83.28% and 83.92%, respectively. The DER is used to measure the difference in decay at different energy levels; due to the photoelectric effect of calcium, calcium-containing stones decay more strongly at low energy, resulting in a higher dual-energy ratio, which is consistent with established physical theories. Although DEI's AUC was 0.827, its specificity reached 92.71%. Early reports [16] indicated that DEI is reliable in excluding certain types of stones, which means that when used in combination with other DECT parameters, it can effectively help

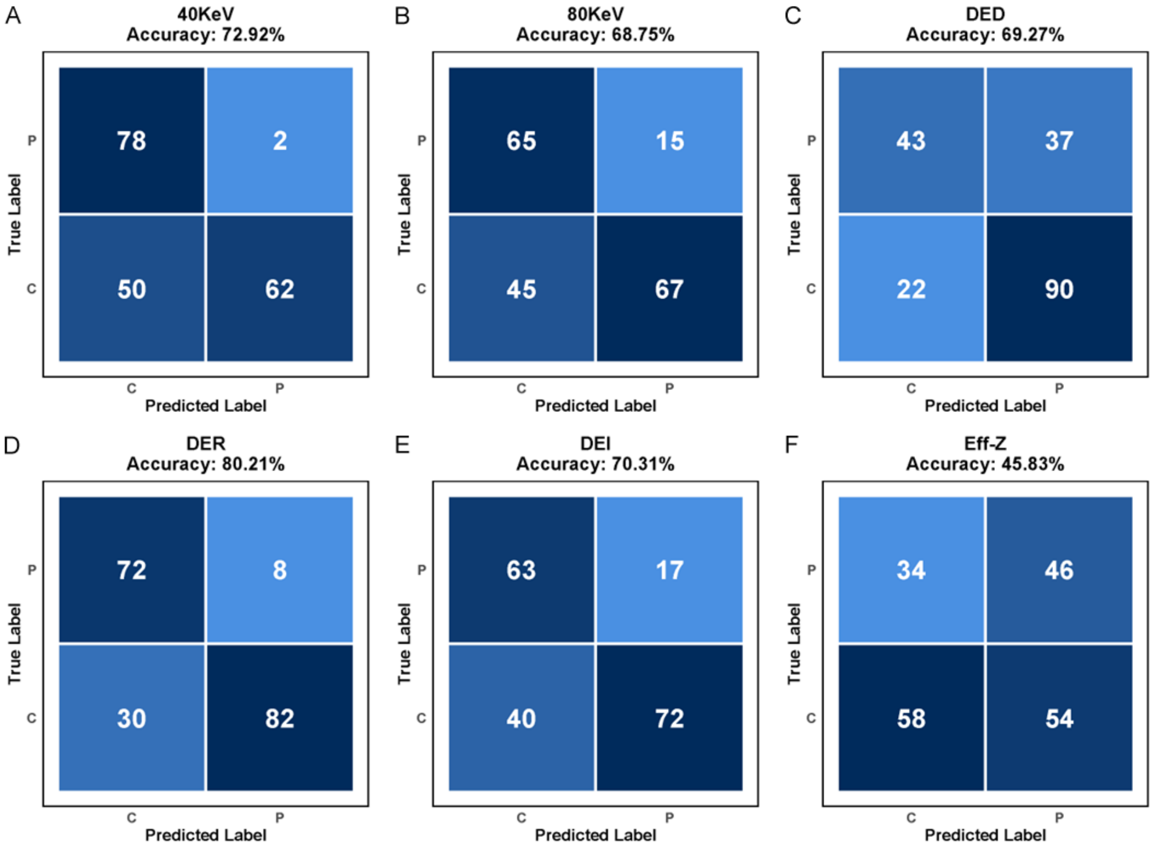

Figure 5. Confusion matrices of dual-source CT parameters for COM stones (C) versus non-COM stones (P). A: Prediction results for 40KeV (Accuracy =72.92%). B: Prediction results for 80KeV (Accuracy =68.75%). C: Prediction results for DED (Accuracy =69.27%). D: Prediction results for DER (Accuracy =80.21%). E: Prediction results for DEI (Accuracy =70.31%). F: Prediction results for Eff-Z (Accuracy =45.83%). Note: DED: Dual Energy Density, DER: Dual Energy Ratio, DEI: Dual Energy Index, Eff-Z: Effective Atomic Number, C: COM Stone, P: Non-COM Stone.

Table 6. Diagnostic performance comparison of dual-source CT parameters in differentiating COM from non-COM stones

Parameter	AUC	CI_lower_upper	Accuracy	Sensitivity	Specificity	Precision	Recall	F1-Score	Cut_off
40 KeV	0.698	0.620-0.776	0.7292	0.9750	0.5536	0.6094	0.9750	0.7500	2657.13
80 KeV	0.685	0.609-0.760	0.6875	0.8125	0.5982	0.5909	0.8125	0.6842	976.96
DED	0.632	0.548-0.716	0.6927	0.5375	0.8036	0.6615	0.5375	0.5931	328.655
DER	0.854	0.800-0.909	0.8021	0.9000	0.7321	0.7059	0.9000	0.7912	1.665
DEI	0.76	0.694-0.827	0.7031	0.7875	0.6429	0.6117	0.7875	0.6885	0.105
Eff-Z	0.549	0.466-0.632	0.4583	0.4250	0.4821	0.3696	0.4250	0.3953	13.245

Note: DED: Dual Energy Density, DER: Dual Energy Ratio, DEI: Dual Energy Index, Eff-Z: Effective Atomic Number, COM: Calcium Oxalate Monohydrate.

exclude UA stones and enhance diagnostic accuracy. In the more challenging task of identifying COM stones, DER showed the best performance, with an AUC of 0.854. COM stones are the most common subtype of calcium oxalate stones, with the highest density and hardness. Bharati et al. [17] reported that the Eff-Z and electron density parameters can distinguish calcium-containing stone subtypes, showing spectral differences compared to mixed calcium-containing stones. DEI reached an AUC of 0.760 for COM identification, which is low, but still has discriminative value. These results offer a new technical approach for preoperative

Table 7. Comparison of dual-source CT parameters in patients among different compositional types of COM stones

Variable	COM (n=80)	COM+COD (n=22)	COM+CaP (n=37)	COM+COD+CaP (n=53)	Test Statistic	*P*-value
40 KeV	2135.68 [1941.30, 2386.56]	2735.16 [1970.05, 3024.02]	2851.44 [2232.10, 3151.74]	2682.89 [1763.03, 3003.01]	22.803	<0.001
80 KeV	847.88 [750.79, 944.50]	1056.30 [780.38, 1237.20]	1015.65 [896.28, 1151.15]	991.66 [775.33, 1157.07]	19.396	<0.001
DED	342.78±131.83	399.09±76.87	408.14±148.43	384.87±89.38	3.27	0.022
DER	1.49±0.16	1.75±0.19	1.77±0.22	1.72±0.19	31.197	<0.001
DEI	0.09 [0.07, 0.10]	0.11 [0.09, 0.13]	0.12 [0.10, 0.13]	0.11 [0.09, 0.13]	39.695	<0.001
Eff-Z	13.57±1.75	12.91±1.89	13.56±1.72	13.12±1.40	1.474	0.223

Note: DED: Dual Energy Density, DER: Dual Energy Ratio, DEI: Dual Energy Index, Eff-Z: Effective Atomic Number, COM: Calcium Oxalate Monohydrate, COD: Calcium Oxalate Dihydrate, CaP: Calcium Phosphate.

COM identification and hold important clinical significance for the formulation of treatment plans.

Compared with earlier studies, this study has made progress in several important aspects. Although previous studies have demonstrated that DECT can differentiate uric acid stones from calcium-containing stones [18], the Eff-Z achieved an AUC of 0.938 in our DECT cohort, which is higher than that reported in most prior studies. This may be related to the large sample size of 311 patients, which provides stronger statistical reliability, and also to the continuous optimization of technical parameters emphasized by Kriegshauser et al. [16] and Cannella et al. [19], who believe that standardization procedures can improve measurement accuracy. Differences in stone composition in the population may also affect the differences in diagnostic performance. An important contribution of this study is the systematic evaluation of the role of DECT parameters in the identification of COM stones, which makes up for the shortcomings of previous studies that mainly focused on the general differences between UA and calcium-containing stones. In this study, we focused on both the identification of major categories and subtypes. Li et al. [20] also pointed out that spectral CT had the potential to identify specific subtypes (such as phosphate stones), which further supported the clinical value of DECT. This study also provides detailed diagnostic indicators, including accuracy, sensitivity, specificity and precision, providing clinicians with a more comprehensive reference. Such comprehensive evaluation is rare in previous studies, highlighting the methodological advantages of this study.

The findings of this study have clear clinical application value. In terms of treatment planning, reliable preoperative prediction of stone composition offers an essential basis for decision-making. When UA stones are predicted, dissolution therapy can be given priority to help patients avoid invasive procedures, reduce discomfort and lower costs. When COM stones are predicted, due to their high hardness and difficulty in stone fragmentation, this means that more intense lithotripsy settings or surgical intervention should be considered from the beginning. Stone composition also plays an important role in prognosis and recurrence prevention. COM stones have a high risk of recurrence, requiring stricter prevention strategies and more frequent follow-up. Accurate preoperative identification can provide patients with personalized dietary and medication recommendations to reduce the recurrence rate. From the perspective of resource allocation, the non-invasive nature of DECT improves patient acceptance and makes it a promising tool for routine diagnosis. Ogawa et al. [21] also showed that single-source DECT can differentiate stone types and detect phleboliths. Accurate preoperative assessment can optimize treatment plans, reduce unnecessary interventions, improve the success rate of initial treatment, and promote more efficient use of medical resources and cost management.

Despite the favorable results, this study still has several limitations. As a single-center retrospective study, it may be subject to selection bias, and its external validity needs to be verified by multi-center prospective studies. The sample size of some subgroups is relatively small, which may reduce the credibility of statistical conclusions. Differences in equipment from different manufacturers also raise concerns about parameter consistency and standardization, which are issues that need to be addressed before its widespread application. From a technical point of view, the accuracy of measurement for small stones (<5 mm) is still low. Wang et al. [22] showed that contrast agents may affect the detection of stones, and mixed stones with complex composition are still difficult to predict. The placement of the region of interest is subjective to some extent, which may affect reproducibility. These issues need to be further addressed in future studies. Further research should focus on confirming the generalizability of these findings through large-scale, multicenter prospective studies. Li et al. [23] demonstrated the practicality of machine learning in stone composition analysis, pointing out that automated diagnostic algorithms based on artificial intelligence are expected to reduce reliance on operators. Standardized operating procedures and quality control systems are needed to ensure consistency across centers. According to previous reports [24], large-sample spectral CT studies may help to establish more accurate predictive models and discover new combinations of spectral parameters that can improve diagnostic accuracy. Cost-benefit analysis will also be important, providing an economic basis for the wider application of dual-source CT in stone management. Ferrero et al. [25] also pointed out that photon-counting detector CT performs better in distinguishing different types of stones, reflecting the continuous evolution of technology.

Conclusion

This study confirms the value of quantitative parameters of DECT in predicting the composition of urinary tract stones. Eff-Z performs best in distinguishing uric acid stones from calcium-containing stones, with an AUC of 0.938, providing support for non-invasive preoperative assessment. DER also showed strong capability in identifying COM stones, providing a new method for more detailed subtype assessment of calcium-containing stones.

Disclosure of conflict of interest

None.

Address correspondence to: Qiong Zheng, Department of Radiology and Medical Imaging, Lanzhou Petrochemical General Hospital (The Fourth Affiliated Hospital of Gansu University of Chinese Medicine), No. 733, Fuli West Road, Xigu District, Lanzhou 730060, Gansu, China. E-mail: 13893269804@163.com

References

[1] Setthawong V, Srisubat A, Potisat S, Lojanapiwat B and Pattanittum P. Extracorporeal shock wave lithotripsy (ESWL) versus percutaneous nephrolithotomy (PCNL) or retrograde intrarenal surgery (RIRS) for kidney stones. Cochrane Database Syst Rev 2023; 8: CD007044.

[2] Baowaidan F, Zugail AS, Lyoubi Y, Culty T, Lebdai S, Brassart E and Bigot P. Incidence and risk factors for urolithiasis recurrence after endourological management of kidney stones: a retrospective single-centre study. Prog Urol 2022; 32: 601-607.

[3] Trinchieri A. Theobromine for treatment of uric acid stones and other diseases. Arch Ital Urol Androl 2024; 96: 13277.

[4] Maruyama M, Sawada KP, Tanaka Y, Okada A, Momma K, Nakamura M, Mori R, Furukawa Y, Sugiura Y, Tajiri R, Taguchi K, Hamamoto S, Ando R, Tsukamoto K, Takano K, Imanishi M, Yoshimura M, Yasui T and Mori Y. Quantitative analysis of calcium oxalate monohydrate and dihydrate for elucidating the formation mechanism of calcium oxalate kidney stones. PLoS One 2023; 18: e0282743.

[5] Cui HW, Silva MD, Mills AW, North BV and Turney BW. Predicting shockwave lithotripsy outcome for urolithiasis using clinical and stone computed tomography texture analysis variables. Sci Rep 2019; 9: 14674.

[6] Huang J, Hou J, Yang W, Zhan M, Xie S, Li S, Li R, Wu S, He Y, Zhao W, Zhang R, Shan G and Ni W. Automatic kidney stone composition analysis method based on dual-energy CT. Curr Med Imaging 2023; 20: 1-13.

[7] Greffier J, Villani N, Defez D, Dabli D and Si-Mohamed S. Spectral CT imaging: technical principles of dual-energy CT and multi-energy photon-counting CT. Diagn Interv Imaging 2023; 104: 167-177.

[8] Li S, Wei X, Wang L, Zhang G, Jiang L, Zhou X and Huang Q. Dual-source dual-energy CT and deep learning for equivocal lymph nodes on CT images for thyroid cancer. Eur Radiol 2024; 34: 7567-7579.

[9] Kaviani P, Primak A, Bizzo B, Ebrahimian S, Saini S, Dreyer KJ and Kalra MK. Performance of threshold-based stone segmentation and radiomics for determining the composition of

kidney stones from single-energy CT. Jpn J Radiol 2023; 41: 194-200.

[10] Gadzhiev N, Gelig V, Rodionov G, Gauhar V and Zeng G. Metabolic differences in 24-hour urine parameters between calcium oxalate monohydrate and dihydrate kidney stones: a clinical study. Diagnostics (Basel) 2025; 15: 994.

[11] Ibis F, Yu TW, Penha FM, Ganguly D, Nuhu MA, van der Heijden AEDM, Kramer HJM and Eral HB. Nucleation kinetics of calcium oxalate monohydrate as a function of pH, magnesium, and osteopontin concentration quantified with droplet microfluidics. Biomicrofluidics 2021; 15: 064103.

[12] Bouteille C, Pere M, Chelghaf I, Rigaud J, Madec FX, Perrouin-Verbe MA and Loubersac T. Mini-percutaneous nephrolithotomy: Is smaller better for kidney stones in patients with neurogenic bladder? Fr J Urol 2024; 34: 102522.

[13] Rompsaithong U, Jongjitaree K, Korpraphong P, Woranisarakul V, Taweemonkongsap T, Nualyong C and Chotikawanich E. Characterization of renal stone composition by using fast kilovoltage switching dual-energy computed tomography compared to laboratory stone analysis: a pilot study. Abdom Radiol (NY) 2019; 44: 1027-1032.

[14] Rudenko V, Serova N, Kapanadze L, Taratkin M, Okhunov Z, Leonard SP, Ritter M, Kriegmair M, Snurnitsyna O, Kozlov V, Laukhtina E, Arshiev M, Aleksandrova K, Salomon G, Enikeev D and Glybochko P. Dual-energy computed tomography for stone type assessment: a pilot study of dual-energy computed tomography with five indices. J Endourol 2020; 34: 893-899.

[15] Kulkarni NM, Eisner BH, Pinho DF, Joshi MC, Kambadakone AR and Sahani DV. Determination of renal stone composition in phantom and patients using single-source dual-energy computed tomography. J Comput Assist Tomogr 2013; 37: 37-45.

[16] Kriegshauser JS, Paden RG, He M, Humphreys MR, Zell SI, Fu Y, Wu T, Sugi MD and Silva AC. Rapid kV-switching single-source dual-energy CT ex vivo renal calculi characterization using a multiparametric approach: refining parameters on an expanded dataset. Abdom Radiol (NY) 2018; 43: 1439-1445.

[17] Bharati A, Rani Mandal S, Gupta AK, Seth A, Sharma R, Bhalla AS, Das CJ, Chatterjee S and Kumar P. Non-invasive characterisation of renal stones using dual energy CT: a method to differentiate calcium stones. Phys Med 2022; 101: 158-164.

[18] Manglaviti G, Tresoldi S, Guerrer CS, Di Leo G, Montanari E, Sardanelli F and Cornalba G. In vivo evaluation of the chemical composition of urinary stones using dual-energy CT. AJR Am J Roentgenol 2011; 197: W76-83.

[19] Cannella R, Shahait M, Furlan A, Zhang F, Bigley JD, Averch TD and Borhani AA. Efficacy of single-source rapid kV-switching dual-energy CT for characterization of non-uric acid renal stones: a prospective ex vivo study using anthropomorphic phantom. Abdom Radiol (NY) 2020; 45: 1092-1099.

[20] Li X, Huang X, Ouyang L, Ma H, Chen H and Li X. The characterization of in vivo urinary phospate stones by spectral CT. Urolithiasis 2022; 51: 10.

[21] Ogawa N, Sato S, Ida K, Kato K, Ariyoshi Y, Wada K, Nasu Y and Kanazawa S. Evaluation of urinary stone composition and differentiation between urinary stones and phleboliths using single-source dual-energy computed tomography. Acta Med Okayama 2017; 71: 91-96.

[22] Wang J, Qu M, Duan X, Takahashi N, Kawashima A, Leng S and McCollough CH. Characterisation of urinary stones in the presence of iodinated contrast medium using dual-energy CT: a phantom study. Eur Radiol 2012; 22: 2589-2596.

[23] Li X, Tang P, Liang F, Wang L, Huang X, Li J and Zhen X. Machine learning based multi-label classification of single or mixed-composition urinary stones in in vivo spectral CT. Med Phys 2023; 50: 661-674.

[24] Li X, Wang LP, Ou LL, Huang XY, Zeng QS and Wu WQ. Revolution spectral CT for urinary stone with a single/mixed composition in vivo: a large sample analysis. World J Urol 2021; 39: 3631-3642.

[25] Ferrero A, Gutjahr R, Halaweish AF, Leng S and McCollough CH. Characterization of urinary stone composition by use of whole-body, photon-counting detector CT. Acad Radiol 2018; 25: 1270-1276.